PROGRESS REPORT, 2006-2007

Investigation of Novel Schemes for Injection/Extraction Kickers (LCRD 2.22)

Personnel and Institution that had requested funding

University of Illinois at Urbana-Champaign, Department of Physics:
George D. Gollin, Michael J. Haney, Joseph Calvey, Jason Chang, Michael Davidsaver, William Dluger, Chang Lee

Collaborators

Fermi National Accelerator Laboratory:
David A. Finley, Chris Jensen, Vladimir Shiltsev

Cornell University, Department of Physics:
Gerald F. Dugan, Mark Palmer, David L. Rubin

Project Leader

George Gollin
g-gollin@uiuc.edu
(217) 333-4451

Project Overview

The 2820 bunches of an ILC pulse would require an unacceptably large damping ring if the 337 ns linac bunch spacing were used in the damping ring. As a result, the TESLA 500 GeV design[1] called for 20 ns bunch separation in a 17 km circumference damping ring; a kicker system would deflect individual bunches on injection or extraction, leaving the orbits of adjacent bunches in the damping ring undisturbed. Faster kickers would allow the operation of smaller damping rings, and progress on kicker technologies has been rapid.

The ILC Reference Design Report[2] was released by the Global Design Effort early in 2007. It calls for 6.7 km circumference rings using "conventional" stripline kickers driven by fast HV pulsers. But "because Fourier pulse-compression kickers provide a

[1] *TESLA Technical Design Report*, http://tesla.desy.de/new_pages/TDR_CD/start.html (March, 2001).
[2] *International Linear Collider Reference Design Report 2007*, http://media.linearcollider.org/rdr_draft_v1.pdf , February 7, 2007.

very different approach, it is worthwhile continuing studies to develop a more complete understanding of the benefits and limitations of these systems."[3]

We have been working on both approaches to fast kickers, studying stripline kickers using the 16 MeV electron beam available at Fermilab's AØ photoinjector facility, as well as modeling a Fourier series kicker module that could be built in collaboration with the FNAL RF group. Our initial goals were to determine the suitability of the AØ beam for precision kicker studies and to model variations on the original Fourier series kicker concept. Because Cornell and KEK are also conducting kicker studies (primarily focused on stripline devices) it is appropriate for us to put some attention on alternative approaches that are outside the scope of the Cornell and KEK investigations.

Progress Report: stripline kicker studies using Fermilab's AØ 16 MeV e^- beam

Stripline kicker

Engineers in Fermilab's Technical Division designed and built a stripline kicker for us in 2005. The device's parallel electrodes are approximately 26 cm long and separated by 1 cm. The electrodes form a 100 Ω transmission line which contains the kicking electric and magnetic fields. Two high voltage pulses of opposite polarity travel through coaxial hardline cables to enter the kicker vacuum vessel through HV feedthroughs attached to the electrodes. The pulses propagate along the electrodes in the upstream direction, leaving the kicker through another pair of feedthroughs to travel through standard coaxial cables that are properly terminated. Photographs of the partially assembled kicker are presented in Figure 1.

Design of the kicker was guided by detailed simulation of the device's electrodynamic properties, included the modeling of the electrode support structure and vacuum vessel. Initial studies employed an available high voltage pulser with the relatively slow rise time of 10 ns but we also used a faster commercial pulser purchased by Cornell. This device was identified as a "FID Pulser" according to the label on its case. We had expected that the device would use a Fast Ionization Dynistor (FID) switch. To all of our surprise, the pulser was designed around a non-FID FET switch.

Kicker electrode simulations showed that close attention to the geometry of the electrode support structure was important. In particular, the capacitive path from the electrodes to the wall of the vacuum vessel provided by the posts holding the electrodes determined the frequency of a resonance that could cause signals to be reflected from the HV feedthroughs, rather than entering the vacuum vessel.

---

[3] *Recommendations for the ILC Damping Rings Baseline Configuration,* http://www.desy.de/~awolski/ILCDR/DRConfigurationStudy_files/DRConfigRecommend.pdf, draft dated December 20, 2005.

Figure 1. Kicker assembly. Left photo: electrodes, visible inside the vacuum vessel. Right photo: installing ion pumps.

Three different support structure geometries, labeled with the frequencies of their associated resonances, are shown in Figure 2. The frequency dependence of the reflection coefficients for these structures is shown in Figure 3. (Recall that a rise time of 1 ns corresponds to a frequency of about 0.5 GHz.) The version actually constructed is thought to behave similarly to the 2003 MHz version.

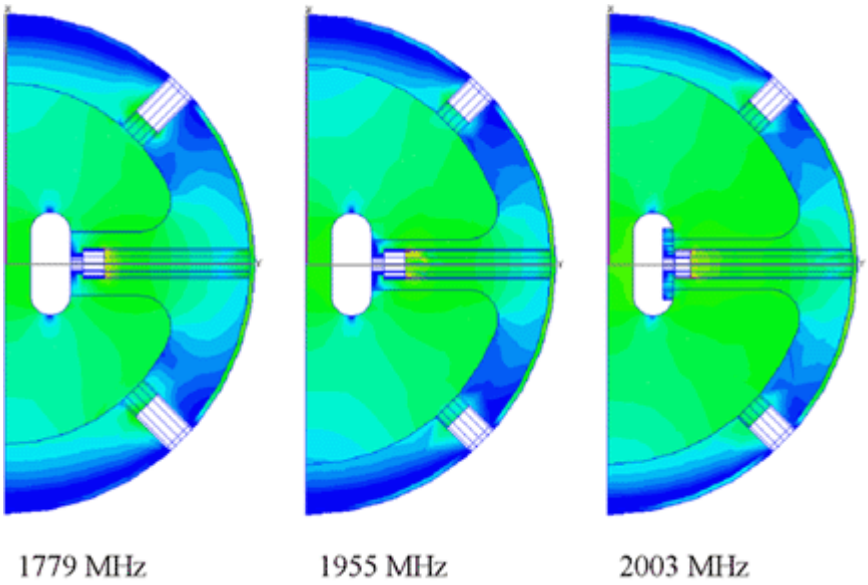

Figure 2. Study of the resonance properties of different electrode support geometries.

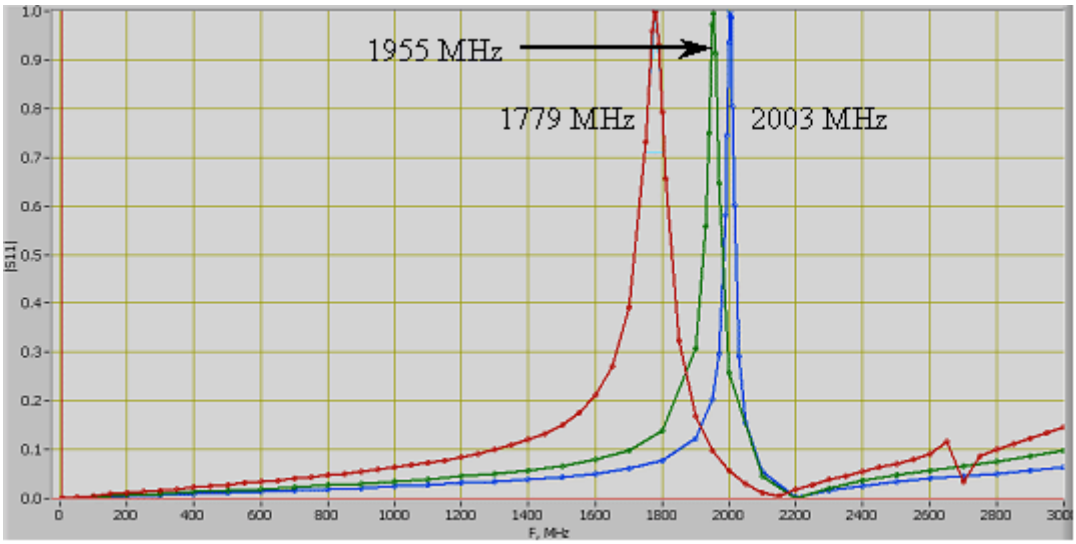

Figure 3. Frequency dependence of the reflection coefficients for the structures shown in the previous figure.

The “FID pulser” delivered ±1 kV pulses to the kicker electrodes. The pulser’s output, measured at the pulser immediately after a high-power attenuator, is shown in Figure 4. The pulse rise and fall times are approximately one and three nsec respectively.

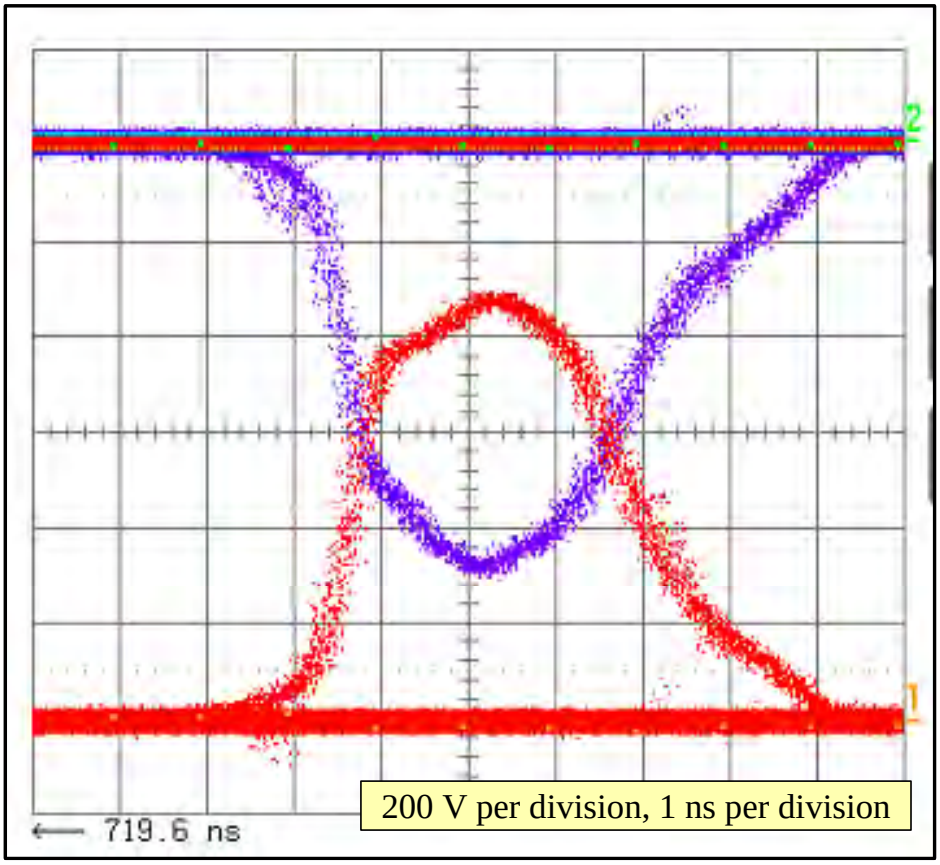

Figure 4. High voltage pulser outputs. We used this pulser to excite the kicker.

Fermilab's AØ 16 MeV electron beam

The AØ beamline in the vicinity of the kicker is shown schematically in the diagram of Figure 5. The beamline was instrumented with beam position monitors, a small steering magnet immediately downstream of the kicker, and a dipole spectrometer magnet. The kicker after installation at AØ is shown in Figure 6.

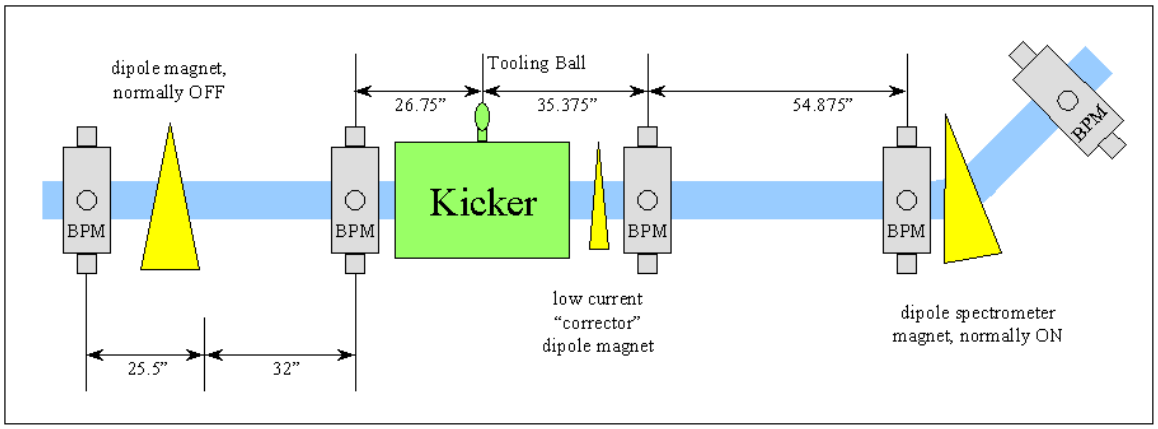

Figure 5. Approximate layout of the AØ beamline.

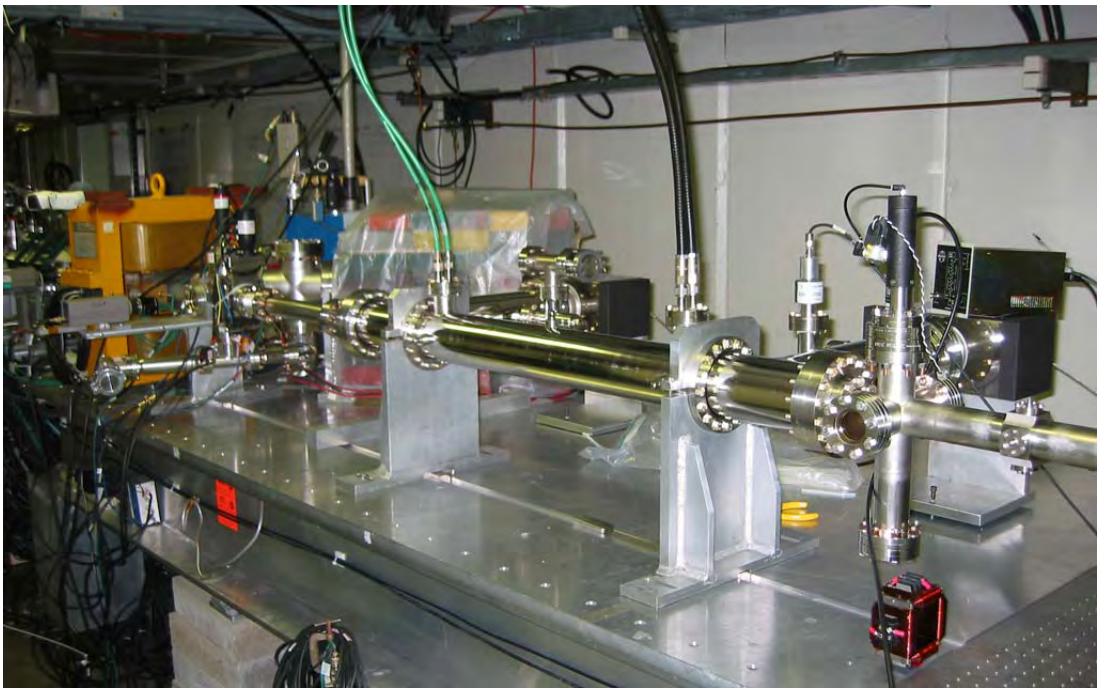

Figure 6. Looking upstream in the AØ beamline after installation of the kicker. High voltage pulses enter the kicker through the black cables visible near the downstream end of the kicker.

A "phase detector" (a small cavity in the beamline several meters upstream of the kicker) provided us with beam-induced signals that were mixed with the beamline's 1.3 GHz master timing signal to determine the arrival time of electron bunches to a precision that we estimate to be ~5 ps.

Data at AØ

We installed the kicker and built a working data acquisition system during 2005, taking data for the first time in August 2005 and then again in 2006. An event display in which the kicker deflects the beam to the right, while the corrector magnet compensates with a left bend, is shown in Figure 7.

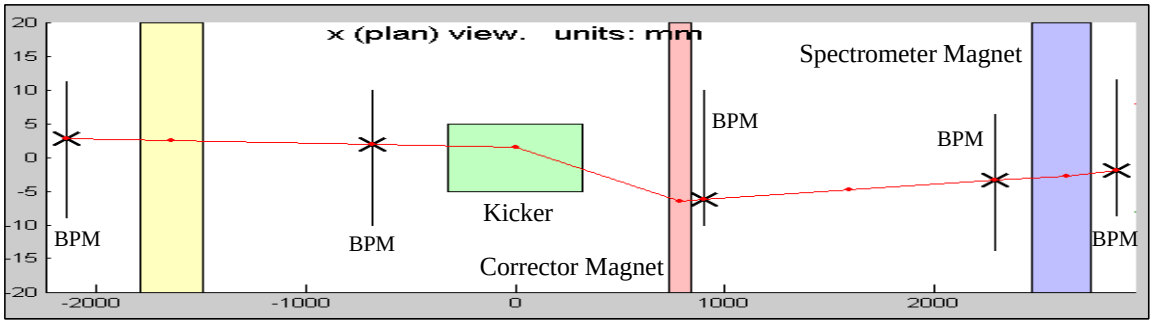

Figure 7. Event display of one event.

Samples of what we work with are shown in Figure 8. The "lego plot" on the left represents the illumination profile in the BPM that is downstream of the spectrometer magnet. The oscilloscope traces on the right show signals from the kicker electrodes and phase detector. Normally the electrode signal displays the HV pulse, but in this particular run we had turned the HV supply off for alignment purposes. The negative pulses that feature prominently illustrate the response of the electrodes to the passage of a beam bunch. The phase detector oscillations induced by this pulse are shown in the third trace. The positions of peaks and zero-crossings in this trace allow us to determine the time of the bunch's passage to an accuracy of about five picoseconds.

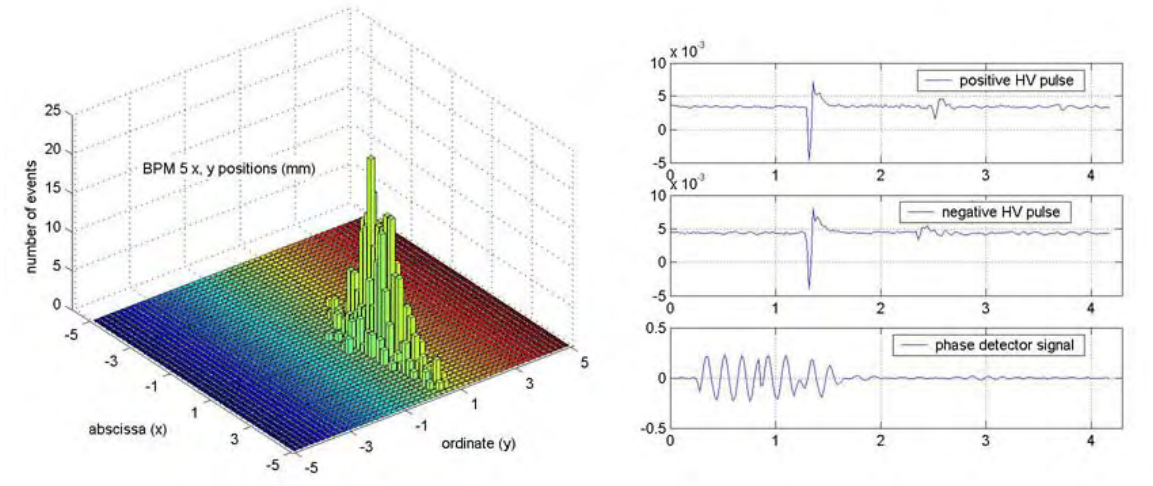

Figure 8. Data from AØ: beam profile in the last BPM (left); oscilloscope traces showing kicker electrode pickup of a passing bunch as well as induced oscillations in the "phase detector."

Phase detector signals, after down-mixing to 60 MHz, are shown in Figure 9. Because the down-mixing process preserves phase information present in the original 1240 MHz

signal from the phase detector, our precision in determining the time of excitation of the phase detector is 1240 MHz / 60 MHz = 20.7 times more accurately than the scale in Figure 9 might naively suggest.

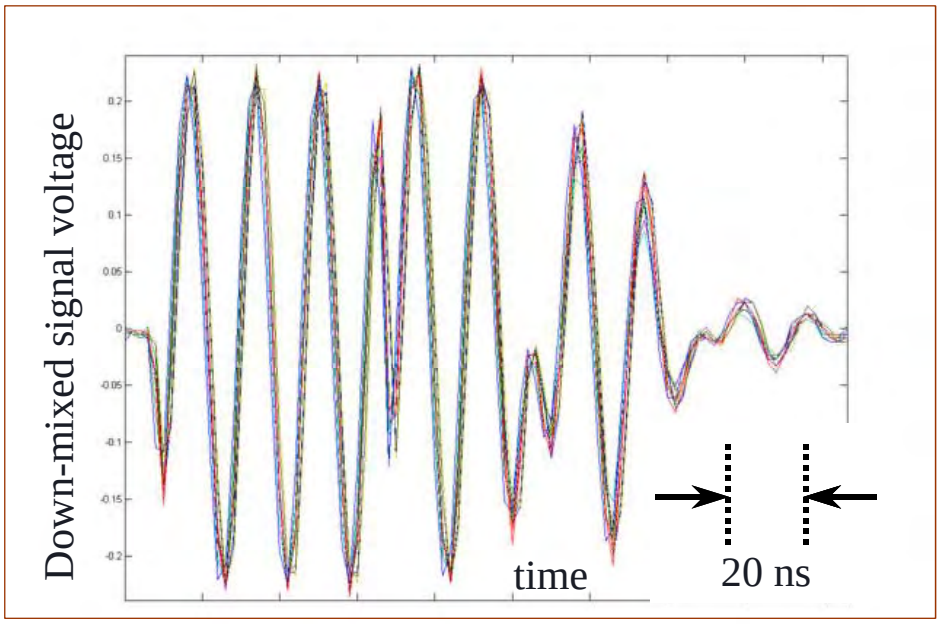

Figure 9. Down-mixed phase detector signals from several events. The phase detector signal excites a 1240 MHz resonant structure. This 1240 Hz signal is mixed with the AØ 1300 MHz master RF signal to produce the ~60 MHz signal recorded with event data, and displayed in the Figure.

Some results

We installed the kicker and built a working data acquisition system during 2005, taking As shown in Figure 10, we found that the time difference between the positive and negative HV pulses sent to the kicker varied by ~100 ps or less. This 70 ps figure includes both resolution of the digital oscilloscope used to capture timing information and any jitter caused by the FID itself. Note that the phase detector does not play a role in this determination.

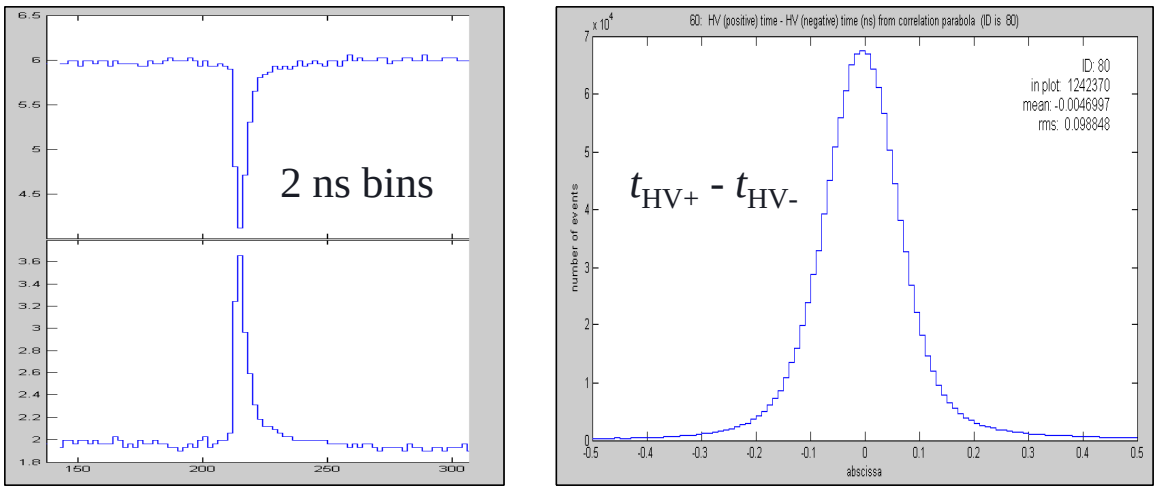

Figure 10. HV pulses from the FID pulser. The time difference shown in the right-hand graph includes jitter in the FID as well as measurement uncertainty in the digital oscilloscope used to obtain event data.

We found the variation in time delay between the FID HV pulse and the raw phase detector signal after down-mixing (this is the signal shown in Figure 9) to be 375 ps. If we ascribe all of this to variations in bunch arrival time at the phase detector relative to the 1300 MHz master AØ clock, we would conclude that AØ electron bunches exhibit shot-to-shot jitter of approximately 18 ps, since the phase detector signal written with event data is down-mixed from 1240 MHz to 60 MHz. If other sources of error contribute, the AØ shot-to-shot jitter will be less than 18 ps. (See Figure 11.) If, instead, we assume that the FID is the primary cause of the RMS width observed in Figure 11, then we would conclude that the shot-to-shot timing jitter of the FID is about 375 ps.

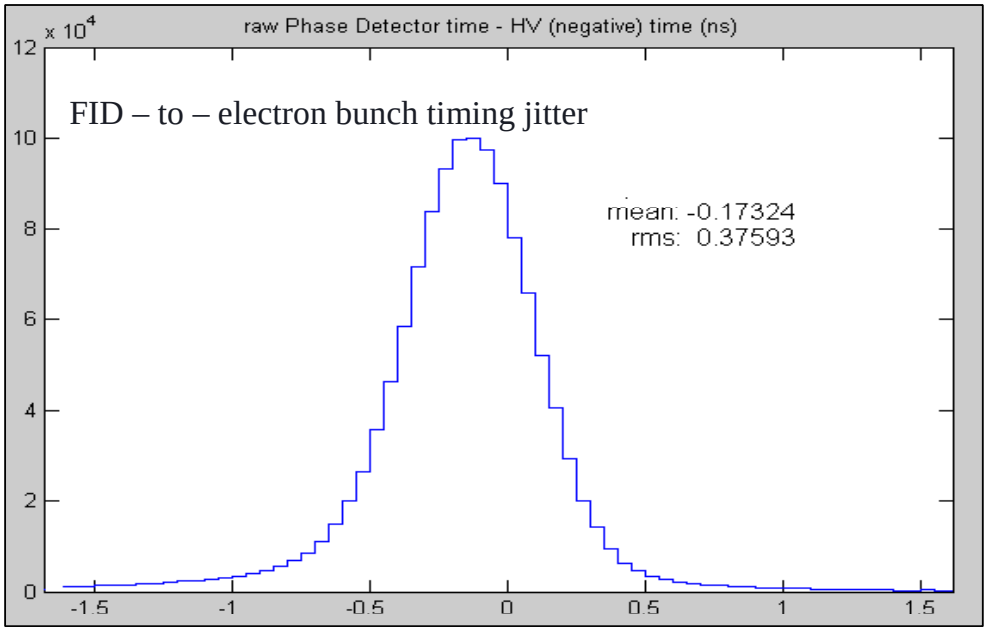

Figure 11. Jitter between raw phase detector signals and FID HV pulses has an RMS width of ~375 ps. If all of this is due to bunch arrival time variations it would correspond to ~18 ps jitter in bunch arrival times. (Less if there are other sources of jitter such as the FID trigger circuitry.) If the FID is the primary cause of the RMS width observed in this Figure 11 we would conclude that the shot-to-shot timing jitter of the FID is about 375 ps.

Since our beamline includes a spectrometer magnet between the last two beam position monitors we are able to analyze the average electron momentum in a bunch on a shot-to-shot basis. As is evident in Figure 12, we find that this quantity varies by about 0.3% from pulse to pulse. The momentum analysis algorithm takes the spectrometer magnet's trapezoidal pole faces into account when determining bunch momentum.

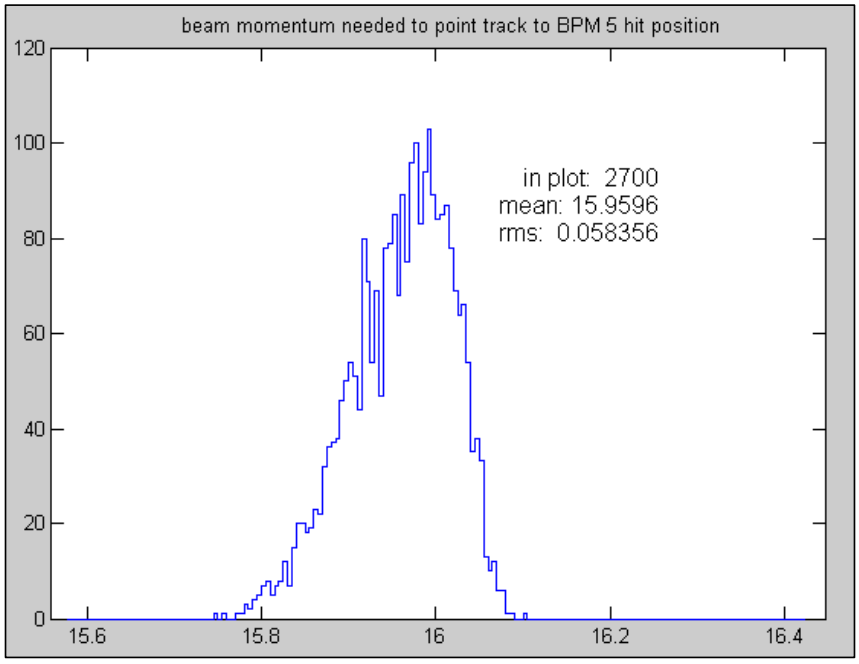

Figure 12. Beam momentum for straight-through events (kicker off, corrector magnet off).

The beam momentum does not vary smoothly with time. Average bunch momentum for 100 consecutive bunches during a straight through run of an hour's duration is shown in Figure 13.

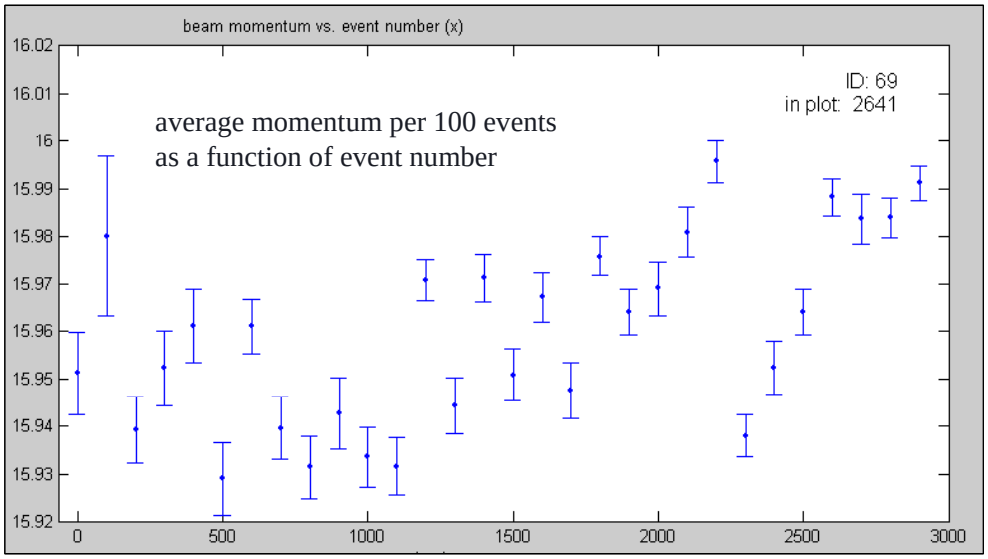

Figure 13. Average beam momentum per 100 events during one straight-through run.

We found that fringe fields from the spectrometer magnet were difficult to take into account in our momentum analysis. These fields caused noticeable steering of the beam

trajectory a fair distance upstream of the spectrometer magnet in spite of all our attempts at installing magnetic shielding to prevent this. The low beam momentum exacerbated the problem posed by fringe fields. In addition, the low beam momentum made it necessary to buck the kicker's impulse with a compensating magnet installed immediately downstream of the kicker. This further complicated our analysis.

It is very convenient to use the AØ photoinjector beam as a drop-in facility for testing instrumentation. However, the complications of analyzing tracking data in such a low energy beam need to be taken into account when planning future tests in AØ. It is likely that fringe fields (primarily from the spectrometer magnet) in combination with variations in beam position contribute significantly to the difficulties in performing a ballistic alignment of the BPM system.

Progress Report: Fourier series kicker studies and other speculative technologies

Fourier series kickers

We described our modeling of a Fourier series pulse compression kicker in detail in the 2006 edition of *A University Program.…*[4] A general discussion of a Fourier-series kicker system can also be found on the web.[5] We have focused on a particular implementation in which an RF amplifier would send a broadband signal down a waveguide to a $Q \approx 25$ RF structure. Dispersion in the waveguide would shift the relative phases of the Fourier components of the signal so that it is compressed: RF power arrives at the RF structure in short, periodic bursts, filling it in order to eject the target bunch without disturbing adjacent bunches. The RF structure is able to store energy, so its maximum field strength would be approximately 20 times greater than the maximum field strength in the downstream end of the waveguide. A schematic representation of the kicker is shown in Figure 14. Our studies assumed the values for the kicker's parameters shown in Table 1.

[4] *A University Program of Accelerator and Detector Research for the International Linear Collider (vol. III),* G.D. Gollin, editor, pp. 116–157, April, 2005. (Available on the web at http://www.hep.uiuc.edu/LCRD/LCRD_UCLC_proposal_FY06/.

[5] George D. Gollin and Thomas R. Junk, *Speculations About a Fourier Series Kicker for the TESLA Damping Ring,* http://www.hep.uiuc.edu/home/g-gollin/Linear_collider/fourier_series_kicker.pdf (2002).

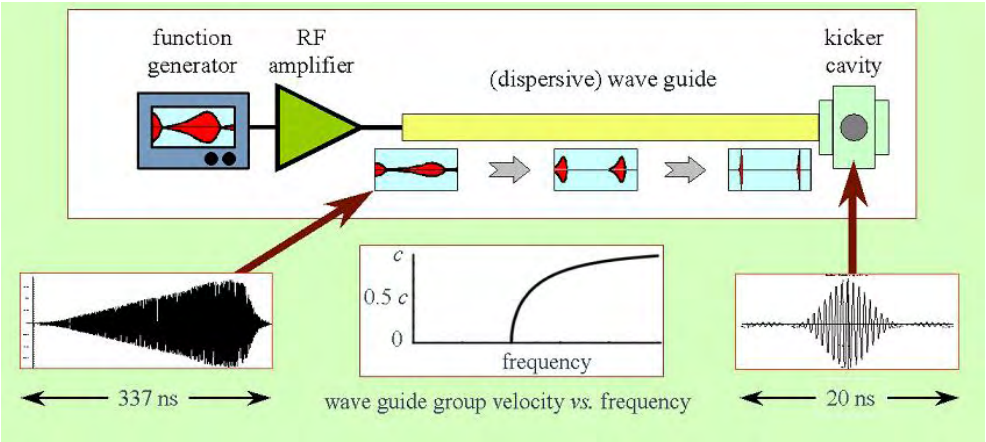

Figure 14: Schematic representation of a Fourier series pulse compression kicker.

Parameter	Symbol	Value
Main linac bunch frequency	f_L ($\omega_L \equiv 2\pi f_L$)	3 MHz
Damping ring bunch frequency	f_{DR} ($\omega_{DR} \equiv 2\pi f_{DR}$)	180 MHz
RF structure center frequency	f_{RF} ($\omega_{RF} \equiv 2\pi f_{RF}$)	1845 MHz
Fourier components in the impulse function		1845 MHz ± 180 MHz
Spacing between adjacent components		3 MHz
RF structure Q	Q	25
Waveguide cutoff frequency	f_{cutoff}	1300 MHz
On field integral	$A(0)$	(100 ± .07) Gauss-meters
Off field integral	$A(t)$	(0 ± .07) Gauss-meters
f_{DR}/f_L	N	60
f_{RF}/f_{DR}	Γ	10.25
f_{RF}/f_L	ΓN	615
Bunch length	δ_B or τ_B	±6 mm ~ ±20 ps

Table 1: Fourier series pulse compression kicker parameters.

The kicker's field integral is a function of time, naturally. We use the term "major zero" to refer to the kicker's (zero-valued) field integral when an unkicked bunch passes through the device. Since the bunch spacing in a train is uniform, the time interval between major zeroes is the same as the interval between the kicking impulse and the first major zero.

We had been considering an impulse function of the following form:

$$A(t) = \frac{1}{N^2}\frac{\sin^2\left(\frac{1}{2}\omega_{DR}t\right)}{\sin^2\left(\frac{1}{2}\omega_L t\right)}\cos\left(\omega_{RF}t\right) = \frac{1}{N^2}\frac{\sin^2\left(\frac{1}{2}N\omega_L t\right)}{\sin^2\left(\frac{1}{2}\omega_L t\right)}\cos\left(\Gamma N\omega_L t\right).$$

An appealing feature of this function is that both the function and its first derivative are zero at all zeroes in the $\sin^2$ numerator except for the special case at $t = 0$. This eliminates

the residual impulse that might be given to the head (or tail) of a bunch passing through the kicker during a zero in impulse that was not paired with a zero first derivative.

Our kicker simulations indicated that the most significant issue to be addressed would be a third-order nonlinear effect. We found that second-order terms at approximately twice the signal frequency (caused by harmonic distortion and intermodulation distortion) could mix with amplifier noise to produce an in-band contribution that cannot be eliminated through adjustment of the initial function generator's program. It is difficult to evaluate the ultimate impact of this effect without building a prototype device.

Pulse compression in a Fourier series kicker

The primary motivation for installing a pulse compression system between the RF amplifier and the kicking cavity and is to permit the use of an amplifier whose peak power and average power were not significantly different.

The kicker could use a pulse compression system that relies on dispersion in a rectangular waveguide transporting power from an amplifier to the kicker's RF structure. Dispersion in the waveguide compresses the amplifier signal: the group and phase velocities for signals propagating down a waveguide with cutoff frequency f_{cutoff} are

$$v_g = c\sqrt{1-\left(f_{cutoff}/f\right)^2} \text{ and } v_\phi = c^2/v_g \ .$$

This would allow an appropriately shaped signal to undergo an evolution of the relative phases of its different frequency components as it traveled down the waveguide, effecting the pulse compression.

The frequency spectrum of the impulse function under consideration was 1845 ± 180 MHz. A waveguide tuned to provide roughly 4° of phase shift per meter between adjacent Fourier components would work as a compressor if built to a length of ~80 meters.

Pulse compression using a lossless "all-pass" filter

We investigated the feasibility of an alternative scheme for pulse compression that would be based on a chain of lossless "all-pass" filters. The filters would introduce a frequency-dependent phase shift that could be used in place of a dispersive wave guide. This work formed the basis of Chang Lee's undergraduate physics thesis. Since it is possible to fabricate RF *LC* filters using printed circuit board technology, it is conceivable that one could fabricate a multi-stage filter as a pulse compressor this way.

A diagram of one type of (passive) all-pass filter is shown in Figure 15. At high frequencies most current flows through the capacitors so V_{in} and V_{out} are in phase. At low frequencies the current path is through the inductors so V_{in} and V_{out} differ in phase by 180°. The details of the filter's behavior will depend on the nature of the load impedance attached to the filter's output, but the general principle is straightforward. For large load

impedance the filter's phase shift will pass through 90° when the impedances of the capacitors and inductors are equal, at an angular frequency given by $\omega^{-2} = LC$.

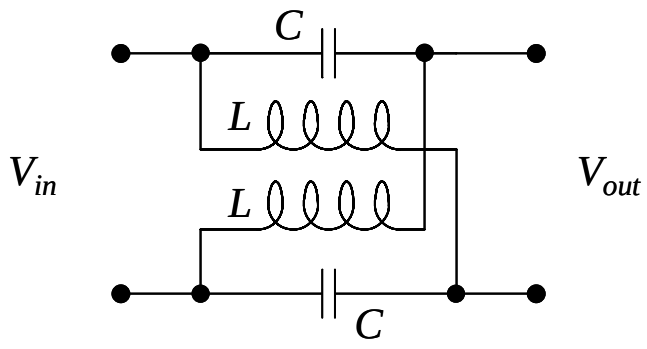

Figure 15: One stage all-pass filter

A single stage filter will not have a particularly sharp effect on the phase of adjacent frequency components in a Fourier series kicker. As is evident in Figure 16 for a filter tuned to 90° at 10 kHz[6], the phase shift per octave is approximately 33° at its steepest point.

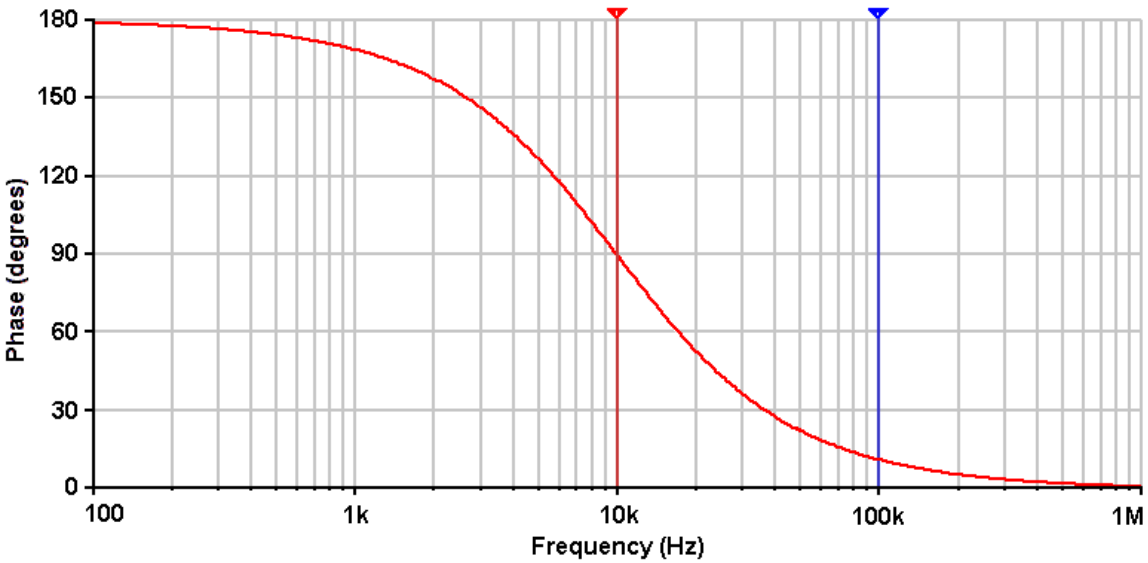

Figure 16: Phase shift vs. frequency for an all-pass filter[6] tuned to 90° at 10 kHz.

Using the parameters in Table 1, we would need to introduce phase shifts of roughly 300 degrees between adjacent Fourier components to obtain adequate pulse compression. This would correspond to a slope in the phase shift vs. frequency curve that is ~4000 times larger than obtained with a single stage filter. We felt it was unrealistic to pursue

[6] http://www-k.ext.ti.com/SRVS/Data/ti/KnowledgeBases/analog/document/faqs/allp.gif

the design of a 4000 stage filter and concluded that all-pass filters did not offer a feasible solution to the compression problem.

A Fourier series kicker without pulse compression

The primary motivation for running a Fourier series kicker at a high harmonic of the damping ring bunch frequency is to allow the full 1845 MHz ± 180 MHz frequency spectrum of the kicking impulse to be contained in a single small, low-Q RF structure. (A number of identical structures would be placed in series to effect the desired transverse kick.)

There are certain advantages to a Fourier series kicker that could run at lower frequencies, supporting f_i = 3 MHz, 6 MHz, … 180 MHz instead. In particular, both the kicking peak and the major zeroes would be sufficiently broad that it would be unnecessary to compensate for slightly different impulses delivered to the head (or tail) and center of a bunch. We felt it would be unreasonably costly to build a system in which each frequency component was loaded into its own resonant structure, with the beam passing through each of these structures. Instead we modeled a system in which a small number of structures were "overmoded," with each being filled with as many frequency components as possible.

It is not possible to construct a long, rectangular cavity that would hold several modes since the boundary conditions do not permit the resonant frequencies to have the right spectrum. In effect, it is the "half-wavelength" condition that the electric field parallel to a cavity surface go to zero at the cavity's walls that spoils the possibility of aligning the mode spectrum with the desired kicking spectrum.

We found that a structure consisting of a pair of long coaxial cylinders could, in theory, be driven to hold multiple modes of the desired frequencies. The "full wavelength" boundary condition in the azimuthal direction, that $E(\phi) = E(\phi+2\pi)$, would permit a series of eight structures of different lengths to hold all 60 Fourier components. As shown in Figure 17, the beam would travel perpendicular to, and below the long axis.

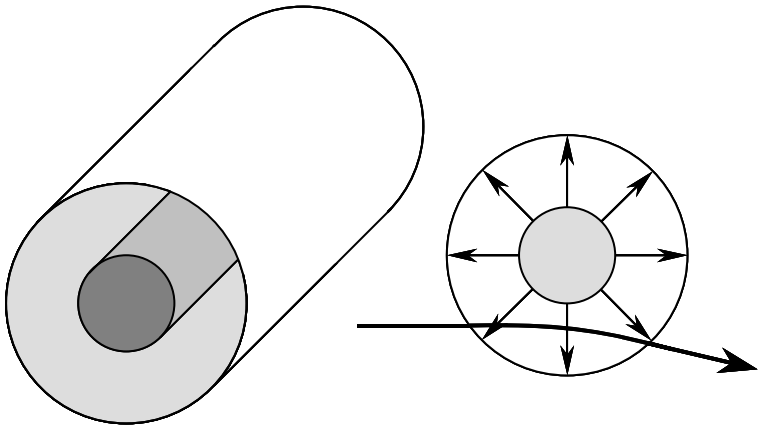

Figure 17: "Organ pipe" coaxial kicking structure

Our modeling of the kicking effects of structures of this sort included an accurate numerical integration of the impulse delivered to the beam. The longest structure would be approximately 50 meters in length, making this a large device!

We did not model the effects on the device's frequency spectrum that insertion of entrance and exit ports for the beam would cause.

We did a few simple bench tests using a long coaxial cable as a model of a kicking structure of this sort and found that we could pump energy into it, measure its *Q*, and understand its other basic properties without difficulty.

Hard disk drive write head technology as a damping ring extraction kicker?

During a visit to UIUC by a researcher from Hitachi Global Storage Technologies, Inc. we learned that a Hitachi hard disk write head can generate a 1 T magnetic field and can reverse the direction of that field in half a nanosecond. The volume in which the field is created is quite small, roughly 120 μm^3, and the disk drive - to - disk drive uniformity of the magnetic field depends largely on the mechanical precision obtained when manufacturing the magnetic parts of the write head. The arm that moves the write head can position the head with great accuracy and reproducibility.

The transverse impulse required to extract a bunch from the damping ring corresponds to a field integral of 1 T·cm so it was interesting to discuss the possibility of using a beefed-up disk drive mechanism as an extraction kicker.

The damping ring transverse bunch size will be very small when the beam is ready for extraction. A transverse aperture of 1200 $\mu m \times 60\ \mu m$ would provide $\pm 3\sigma$ clearance after the beam is fully damped. We imagined that magnet poles of length 1 cm, with pole face separation of 60 μm and pole width of 1200 μm might swing into position after the beam was fully damped. (This will not work if the damping ring beam holds a mix of damped and undamped bunches!)

Hitachi was helpful, and willingly discussed details of the write head mechanism and driver circuitry. Unfortunately, a kicker would need to generate a high quality field of 1 T in a volume of $\sim 720 \times 10^6\ \mu m^3$, approximately six million times larger than that of a disk write head. In that energizing a disk's write head requires a current of approximately 50 mA, filling a small kicker magnet volume with field would require an entirely enormous and impractical current that would be expected to vaporize the mechanism. The scaling from write head to movable kicker magnet does not give cause for optimism!